Imaging Real-Time Proteolysis of Single Collagen I Molecules with an Atomic Force Microscope†

Hai Lin,* Dennis O. Clegg, and Ratnesh Lal

Neuroscience Research Institute and Department of Molecular, Cellular and Developmental Biology, University of California, Santa Barbara, California 93106

Received April 7, 1999; Revised Manuscript Received May 21, 1999

ABSTRACT: The dynamic process of synthesis and degradation of extracellular matrix molecules, including various collagens, is important in normal physiological functions and pathological conditions. Existing models of collagen enzymatic degradation reactions are derived from bulk biochemical assays. In this study, we have imaged in real-time individual collagen I molecules and their proteolysis by *Clostridium histolyticum* collagenases in phosphate-buffered saline (PBS) with atomic force microscopy (AFM). We have also imaged the likely binding and unbinding of collagenase molecules to single triple-helical collagen I molecules and subsequent proteolysis of subsets of the collagen molecules. The proteolysis of collagen molecules was inhibited by reduced calcium and acidification. Results from AFM study of collagen proteolysis are consistent with SDS−PAGE biochemical assays. The real-time proteolysis of single collagen I molecules followed simple Michaelis-Menton kinetics previously derived from bulk biochemical assays. This is the first report of imaging real-time proteolysis of single macromolecules and its inhibition on a molecular scale. A strong correspondence between the kinetics of proteolysis of single collagen molecules and the kinetics of proteolysis derived from bulk biochemical assays will have a wide applicability in examining real-time enzymatic reactions and their regulation at single molecule structural level. Such real-time study of single molecule proteolysis could provide a better understanding of the interactions between proteases and target proteins as well as proteases and protease inhibitors.

The proteolysis of extracellular matrix (ECM) proteins plays a crucial role in many physiological and pathological processes in regulating the integrity of tissue boundaries. Regulated proteolysis is important in cell migration, angiogenesis, immune responses, and tumor cell metastasis (*1*−*3*). Collagens are the major structural components of the ECM, accounting for approximately 25% of total protein in mammals. Collagens are synthesized early in embryonic development and are major constituents of diverse tissue types, such as skin, tendon, blood vessels, cartilage, bone, and basal laminas. Many studies have been carried out to characterize the structural and biochemical properties of collagens, and over 25 collagen subtypes have been identified (*4*). The triple-helical structure of collagen has been studied with X-ray diffraction (*5*) and single collagen molecules have been imaged with electron microscopy (*6, 7*). A variety of bacterial and tissue collagenases (matrix metalloproteinases), and their inhibitors, have been characterized (*1, 3, 8*−*10*).

Proteolysis reactions of collagens by collagenase are typically monitored by SDS−PAGE analysis of end products. However, such studies only provide statistical information regarding population dynamics. Very little information is available for the real-time proteolytic activity of collagenases on individual collagens. More over, there is very little direct three-dimensional (3D) structural information about the binding of collagenase to collagen molecules.

An atomic force microscope (AFM) can be used for real-time and high-resolution imaging of hydrated biological specimens ranging from single molecules to whole cells and tissues (*11*−*13*). AFM has been used to examine interactions between individual macromolecules, such as receptor−ligand and antibody−antigens interactions, DNA hybridization, and protein binding to DNA and RNA (*14*−*17*). Atomic force microscopy has also been used to image single collagen molecules (*18*) and binding of human factor IX to collagen IV molecule at specific sites (*19*).

In the present study, we have imaged individual collagen I molecules, collagen−collagenase complexes, and real-time proteolysis of single triple-helical collagen I molecules by *Clostridium histolyticum* collagenase. Our results provide the first structural images of the proteolysis of single collagen molecules.

EXPERIMENTAL PROCEDURES

Materials. Type I collagen was extracted from rat tail tendon, using method by Brodsky and Eikenberry (*20*), with three rounds of acid solubilization in 0.5 M acetic acid followed by high salt precipitation. Solubilized triple-helical collagen was stored in 0.01 M acetic acid at 4 °C, and purity was confirmed with SDS−PAGE. Purified *C. histolyticum* collagenase (827 U/mg) was purchased from Worthington Biochemical Co. (Freehod, NJ). It is composed of two

* To whom correspondence should be addressed. Neuroscience Research Institute, University of California, Santa Barbara, CA 93106. Telephone: (805) 893−2350. Fax: (805) 893-2005. E-mail:h_lin@lifesci.ucsb.edu.

† Supported by NIH grants EY09736 (H. L.), EY066570(D. C.), GM056290 (R.L) and grants from Santa Barbara Cottage Hospital.

10.1021/bi990800q CCC: $18.00
Published on Web 07/13/1999

separable but very similar collagenases and is free of none nonspecific proteinase activity, according to the manufacturer.

Collagenase Assay. Acid-solubilized collagen I (10 μg) was incubated with 1 μg *C. histolyticum* collagenase (827 U/mg) for 2 h at room temperature in 3 different buffers: (1) PBS containing 1 mM Ca^{2+}, 1 mM Mg^{2+}, pH 7.4; (2) Ca^{2+}- and Mg^{2+}-free PBS with 3 mM EDTA, pH 7.4; (3) PBS containing 1 mM Ca^{2+}, 1 mM Mg^{2+}, pH 4.0. The total volume of the reaction was 50 μL. Electophoresis SDS sample buffer was then added to the collagen/collagenase mixtures and heated for 10 min at 90 °C. The proteins were separated by electrophoresis on 6% sodium docecyl sulfate-polyarylamide gels (SDS−PAGE) under nonreducing conditions (*21*). Prestained molecular weight markers (Biorad, Hercules, CA) were run parallel to the samples. Protein bands were visualized after staining with Coomassie Brilliant Blue R-250 (Biorad, Richmond, CA).

Atomic Force Microscopy. For atomic force microscopy, acid-solubilized rat tendon collagen I was diluted to 1−20 μg/mL in phosphate-buffered saline (PBS) (Life Technologies, Grand Island, NY) containing 1 mM Ca^{2+} and 1 mM Mg^{2+}. Diluted collagen I was absorbed to a freshly cleaved mica surface at room temperature for 1−2 min. The mica surface was then thoroughly rinsed with PBS and imaged by AFM under PBS. The lower concentrations (1−2 μg/mL) of collagen I were only used when we intended to image isolated single collagen I molecules.

For AFM imaging, we used a Nanoscope III Multimode with an Extender electronics module for phase imaging (Digital Instruments, Santa Barbara, CA). All samples were imaged in tapping mode using a D scanner (maximum scan size $\approx$ 11 μm) and silicon nitride tips (200 μm long with nominal spring constant $\sim$0.06 N/m). Multiple driving frequencies between 5 kHz to 80 kHz were tested, and the best images were obtained with a tapping frequency around 28 kHz with a tip oscillating amplitude of 60−120 nm. The scan rates were set between 2 and 3 Hz and the proportional and integral gains were set between 1 and 3. Height and amplitude images, and sometimes along with phase images of the samples, were simultaneously recorded. Images shown in this manuscript were flattened off line and occasionally were zoomed and low-pass filtered using the Digital Instruments Nanoscope III software program in order to highlight specific features.

Perfusion of Collagenase. To image the proteolysis of collagen by collagenase, PBS containing *C. histolyticum* collagenase was perfused on-line, while imaging with AFM, over collagen-coated mica with a peristaltic pump (Rainin Instruments, Emeryville, CA). PBS containing collagenase was perfused for approximately 1 min at a rate of 2 mL/min before perfusion was stopped. This ensured that the fluid covering collagen on mica was replaced with the new perfusion buffer, since the chamber volume is less than 0.1 mL. The samples were continuously imaged during and after fluid change (*22*). Perfusion of fluid introduced noise in the AFM image and often caused the tip to disengage; when this occurred, the tip was immediately re-engaged after the fluid change was completed.

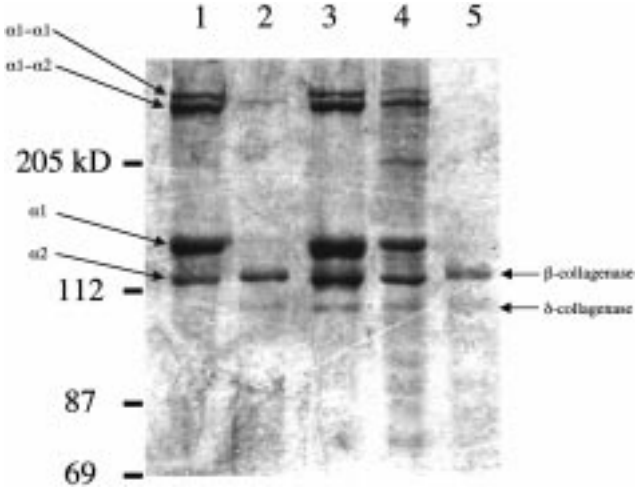

FIGURE 1: Digestion of rat tendon collagen I by *C. histolyticum* collagenases. Samples were separated on a 6% polyacrylamide gel under nonreducing conditions. Collagen I (10 μg) was incubated with *C. histolyticum* collagenases (1 μg) for 2 h at room temperature in PBS with 1 mM Ca^{2+} and 1 mM Mg^{2+} (lane 2), Ca^{2+}- and Mg^{2+}-free medium with 3 mM EDTA (lane 3), and PBS with 1 mM Ca^{2+}, 1 mM Mg^{2+}, pH 4.0 (lane 4). Undigested collagen I (lane 1) and collagenases alone (lane 5) are also shown. Positions of molecular weight markers are indicated on the left.

RESULTS

The proteolysis of collagen I by *C. histolyticum* collagenase was carried out and proteolytic products were analyzed by SDS-PAGE (Figure 1). A triple-helical collagen I molecule is composed of two α1 chains and one α2 chain, and two of the 3 chains are cross-linked. When undigested collagen I is separated on SDS-PAGE, four distinct bands appear (Lane 1): cross-linked α1−α1 and α1−α2 dimers, α1 monomer, and α2 monomer. The purified *C. histolyticum* collagenases separated into two clearly defined bands of size $\sim$115 kD and $\sim$100 kD, which correspond to type β- and δ-collagenase, respectively (Lane 5; (*8*)). Each of the type β- and δ-*C. histolyticum* collagenases makes at least four cleavages on a triple-helical collagen I molecule, all at distinct sites (*10*). In the presence of 1 mM Ca^{2+}, after 2 h of incubation at room temperature, 10 μg of collagen I was completely cleaved into small fragments ($<$60 kD) with no clearly distinguishable bands other than the collagenases (Lane 2). However, in Ca^{2+}- and Mg^{2+}-free medium with 3 mM EDTA, the *C. histolyticum* collagenase activity was almost entirely inhibited (Lane 3). The activity of *C. histolyticum* collagenases also exhibited strong pH dependence collagenase activity was significantly inhibited at pH 4.0 (Lane 4).

When 1−2 μg/mL collagen I was absorbed to a freshly cleaved mica surface for $\sim$1−2 min, many isolated single collagen I molecules were attached to the mica. Figure 2 shows an amplitude mode image of single collagen I molecules imaged in PBS on mica. Single collagen I molecules appear approximately 300 nm long with a height (thickness) of 1−2 nm. These spatial features are consistent with measurements from previous studies (*5*, *18*). The widths of imaged collagen I molecules are between 6 and 14 nm, and this widening is likely due to probe-tip-induced broadening, commonly observed in the images of isolated macromolecules.

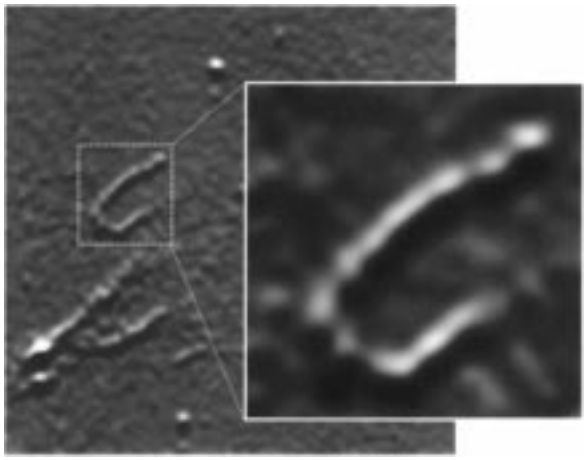

FIGURE 2: Single triple-helical collagen I molecule as imaged by tapping mode atomic force microscope in amplitude mode, three collagen molecules are seen in the left portion of the image. The scanned area is 0.6 μm × 0.6 μm. The inset magnifies one of the collagen molecules. Amplitude mode imaging highlights the leading edge and darkens the trailing edge of the molecules.

When 20 μg/mL collagen was absorbed to freshly cleaved mica for ~1−2 min, significantly more collagen molecules were attached to the substrate. Many collagen molecules appeared to overlap each other and form a random meshwork one to two molecules deep (Figure 3A). AFM imaging of this collagen meshwork showed that collagen I molecules were firmly attached to the mica substrate in PBS and could be imaged in tapping mode for up to 2 h without much alteration in the positioning of the collagen molecules.

The proteolysis of collagen I by *C. histolyticum* collagenases was imaged in real-time. Figure 3 shows results from one such experiment: collagen I molecules were imaged prior to, during, and after 2 μg/mL *C. histolyticum* collagenase was added. PBS containing 2 μg/mL collagense was perfused over collagen-coated mica for approximately 1 min, as indicated by the arrows besides Figure 3B, at a flow rate of 2 mL/min. Four minutes after the addition of collagenase, some collagen I molecules (~40%) were already cleaved (Figure 3C). In Figure 3C, some smaller globular structures began to appear in the image. These structures are likely to be collagenase-digested collagen fragments and collagenase molecules bound to collagen molecules or deposited on mica. After incubation with collagenase for 20 min, the collagen I molecules were almost entirely digested (Figure 3F). The image sequence in Figure 3 represents the best complete sequence obtained in our present study, qualitatively similar sequence of images were obtained in five other similar experiments. When higher concentrations of collagenase (10−100 μg/mL) were added, the collagen degradation was much faster: the collagen I molecules were almost completely degraded in 2 min or less, within a single image frame (data not shown).

Figure 4A and B show an enlarged view of a portion of Figure 3B and C, the time lapse between these images was approximately 4 min. These images clearly show that individual collagen I monomers were cut by collagenases. Some of the digested molecules are indicated by the arrows.

Figure 5A−C show an enlarged view of another portion of images shown in Figure 3A−C. Some globular particles bound to some collagen molecules appeared soon after addition of collagenase, as indicated by the arrows. Many of these particle-bound collagen molecules subsequently broke down at the binding sites (thick arrows). Some of the bound particles dissociated from the collagen molecules (thin arrow). These particles bound to collagen are most likely to be the individual collagenase molecules, which later either dissociated from the collagen molecule or digested the collagen at the cleavage sites.

For comparison, Figure 6 shows a phase-mode image of single *C. histolyticum* collagenase molecules on mica in PBS. In Figure 6, background noise was intensified due to imaging in the phase mode and does not represent collagenase molecules.

C. histolyticum collagenases are Ca^{2+}- and pH-dependent (Figure 1; *23*, *24*). The inhibitory effects of Ca^{2+}-free/EDTA and acidic pH on collagenase reactions were imaged in real-time. When the collagenases (1 μg/mL) were perfused over collagen I in calcium-free (with 3 mM EDTA) buffer, little degradation of collagen molecules was observed even after 30 min (Figure 7A and B) which indicates the calcium-dependent inhibition of proteolysis. Twenty minutes after 1 μg/mL *C. histolyticum* collagenases were reintroduced in PBS containing 1 mM Ca^{2+}, the collagen I molecules on the mica substrate were completely degraded (Figure 7C). When *C. histolyticum* collagenases (1 μg/mL) were incubated with collagen I molecules on mica in PBS at pH 4.0, only a small fractions of collagen I molecules were degraded after 30 min (Figure 8A and B). However, after the pH was raised to 7.4, the collagen molecules were promptly degraded (Figure 8C).

DISCUSSION

In the present study, we have imaged real-time proteolysis of single collagen I molecules by *C. histolyticum* collagenases as well as the likely binding of single collagenases to single collagen molecules and subsequent collagen degradation. The collagen proteolysis was Ca^{2+}- and pH-dependent, consistent with biochemical assays.

Collagen fibers are the fundamental structural elements of extracellular matrix and some tissues. They are resistant to many nonspecific proteinases. Higher organisms produce two types of tissue collagenases (matrix metalloproteinases), namely, the fibroblast-type and the neutrophil-type. Tissue collagenases can degrade collagen fibrils of type I, II, and III interstitial collagens by cutting the triple-helical collagen monomers at a single cleavage site, and splitting the molecules into two fragments, one-fourth and three-fourths of the original length. The intricate dynamic balance between the synthesis of collagen and production of tissue collagenases and collagenase inhibitors has significant implications for physiological functions and many pathological conditions (*1*−*3*).

The bacterium *C. histolyticum* produces at least seven subtypes of different collagenase, all are metalloproteinases. These collagenases are categorized into two different classes, class I and II, according to their sequence homologies and biochemical and proteolytic properties (*8*, *25*). Purified *C. histolyticum* collagenases used in this study contain predominantly a ~115 kD collagenase and a ~100 kD collagense (Figure 1), presumably type β- and δ-collagenases (*8*). Type β-collagenase is a class I collagenase, and δ-collagenase belongs to class II. Unlike tissue collagenase,

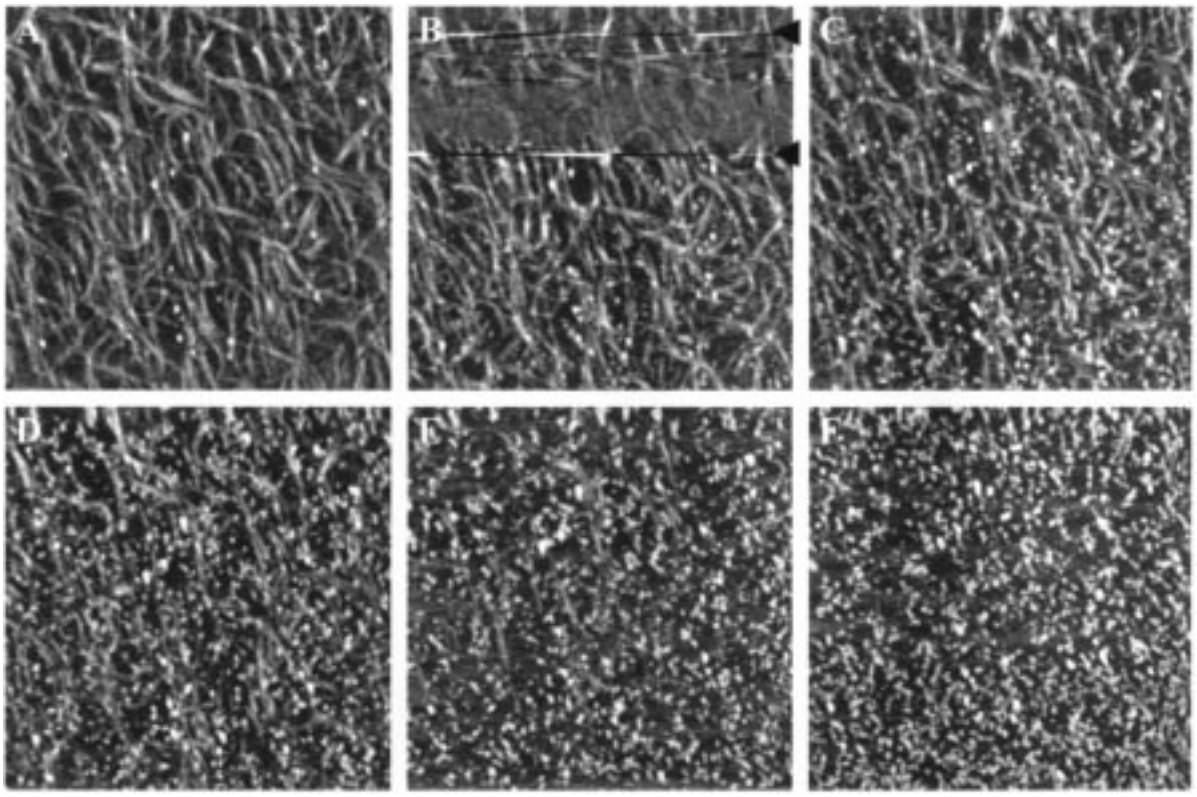

FIGURE 3: Continuous digestion of collagen I by *C. histolyticum* collagenase imaged by tapping mode atomic force microscope in height mode. The images were 512 × 512 pixels, scanned at 2 Hz from top to bottom, and the scanned area is 2 μm × 2 μm. Each image took approximately 4 min to capture. These images show the collagen molecules (A) before addition of collagenase (1 μg/mL), (B) during and immediately after collagenases addition, (C) 4 min, (D) 8 min, (E) 16 min, and (F) 24 min after collagenase was added. The start and stop time for perfusing collagenases were indicated by two arrows in panel Figure 3B.

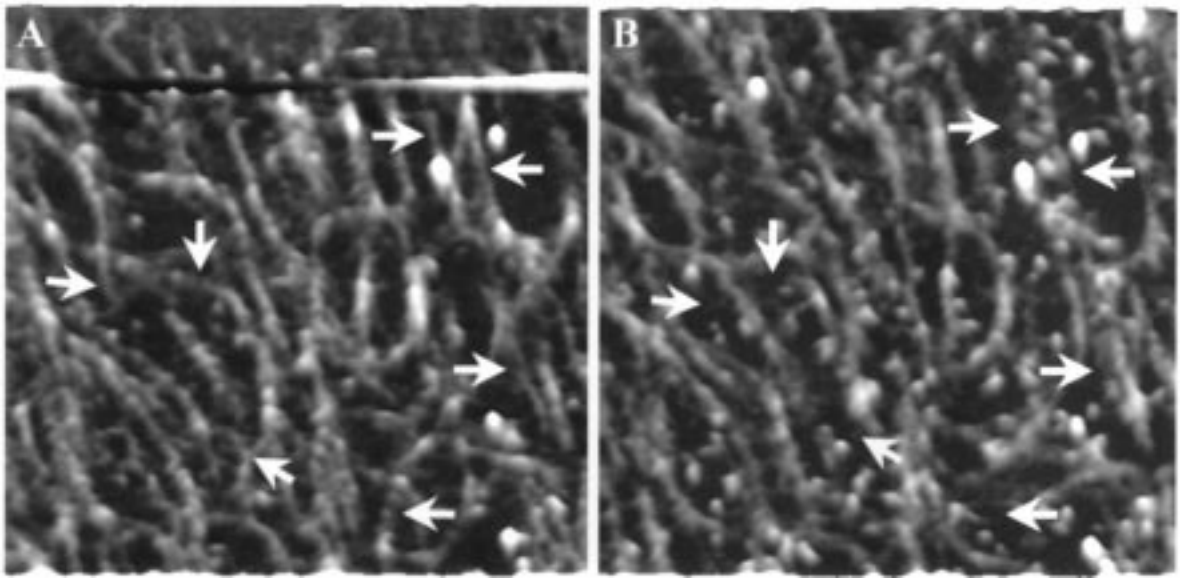

FIGURE 4: A higher magnification view of digestion of single collagen molecules by *C. histolyticum* collagenase (enlargement of middle left portion of Figure 3B and C). (A) Right after collagenase was added, (B) four minutes later. Stoppage of collagenase inflow was visible by the ripple line across the top of (A). A few of the collagen molecules, as some marked by arrows in A) were clearly degraded in (B). Image size: 1 μm × 1 μm.

C. histolyticum collagenases cleave collagens at multiple sites: each of the class I and class II *C. histolyticum* collagenases make at least four cuts on each triple helical collagen I monomer at distinct sites (*10*). Collagen I molecules could eventually be degraded into nine small fragments using both classes of *C. histolyticum* collagenases in our experiments, which is consistent with data shown by the SDS−PAGE in Figure 1 as well as AFM images Figures 3 and 4.

We have observed globular particles bound to triple-helical collagen I molecules immediately after the perfusion of collagenases (in 0−2 min, Figure 5). Although we cannot entirely rule out the possibility that some of these bound particles are cleaved collagen fragments, we concluded that

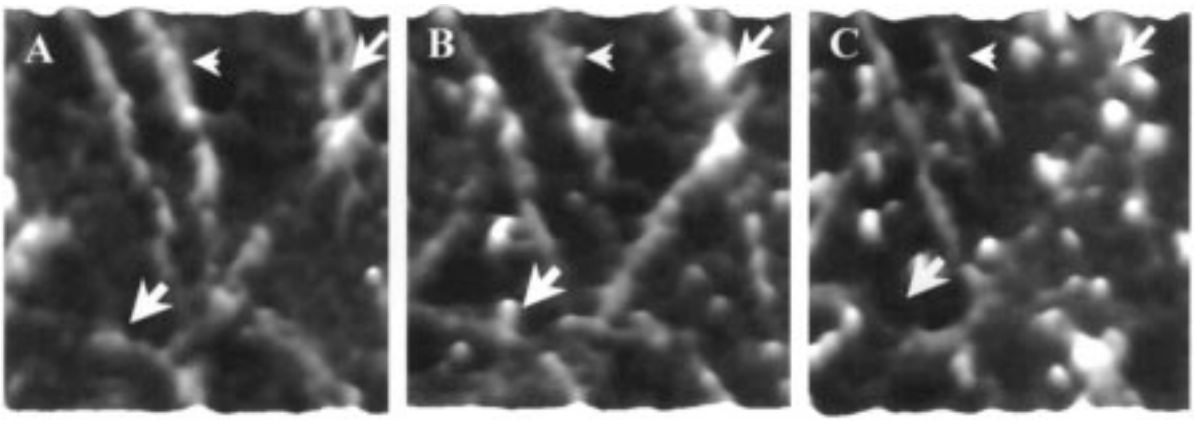

FIGURE 5: Close-up view of collagenase binding to collagen I molecules (enlargement of lower central portion of Figure 3A−C): collagen I molecules (A) before, (B) immediately after collagenase addition, and (C) 4 min later. In (B), three globular particles were bound to collagen molecules as indicated by the arrows, two collagen molecules (thick arrows) were broken at these sites, while one particle (thin arrow) dissociated from collagen 4 min later in C. Image area: 0.6 μm × 0.6 μm.

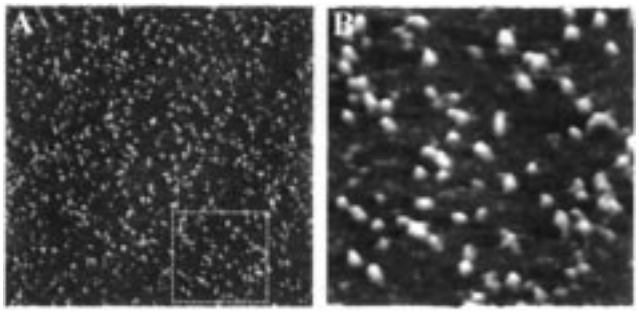

FIGURE 6: Phase mode image of single *C. histolyticum* collagenase molecules on mica in PBS: (A) scan size: 2 μm × 2 μm, a portion (0.6 μm × 0.6 μm) indicated by dashed lines is enlarged and shown in (B). (B) has the same image size as Figure 5A−C. Background noises were intensified due to imaging in the phase mode and do not represent collagenase molecules.

the majority of these particles are collagenase molecules for the following reasons: (1) these collagen-bound particles appeared soon after the addition of collagenase (within 1 min) when little proteolysis of collagen had occurred (Figure 9; (2) most these collagen molecules subsequently broke at the binding sites; (3) the particles are similar in size compared to single collagenase molecules on mica (Figure 6).

C. histolyticum collagenases are metalloproteinases, which require Zn^{2+} and Ca^{2+} for their proteolytic activity (*8*). *C. histolyticum* collagenase activities are inhibited by chelation of Ca^{2+}, and their activity is temperature and pH dependent (*23*, *24*). Our data confirm the Ca^{2+}- and pH-dependent properties of *C. histolyticum* collagenases (Figures 1, 7, and 8). The proteolysis of collagen by *C. histolyticum* collagenase was completely inhibited by the removal of Ca^{2+} (with EDTA, Figures 1 and 7), and this Ca^{2+}-dependent inhibition is reversed when Ca^{2+} was added back (Figure 7C). A previous study showed that at pH∼4.5 *C. histolyticum* collagenase activity was inhibited by approximately 30% compared to neutral pH (*24*); our data (Figures 1 and 8) indicate that at pH 4.0 this inhibition is much more significant (>50%). Such a higher level of inhibition could partly be due to differences in experimental conditions, such as buffer, temperature, etc.

Though tissue collagenases and bacterial collagenases bind different sites on the collagen helix, they have similar kinetic properties in recognizing collagens. For hydrolysis of different types of collagen, The K_m value varies for the hydrolysis of different types of collagen: it is between 2 and 12 μM for various subtypes of *C. histolyticum* collagenases and between 0.82 and 2.6 μM for tissue collagenases. The rate constant of collagen hydrolysis k_{cal} is between 250 and 2100 hr^{-1} for *C. histolyticum* collagenases and 3.2−350 hr^{-1} for tissue collagenases (*9*, *26*, *27*). Type β *C. histolyticum* collagenase activity is temperature dependent, it has K_m = 4−12 μM and k_{cal} = 500−2100 hr^{-1} for hydrolysis of soluble rat type I collagen, and at 25 °C, K_m ≈ 4 μM and k_{cal} ≈ 1000 hr^{-1}. Kinetic parameters for type δ-collagenase are not currently available, but other class II (types ϵ and ζ) collagenases have very similar kinetic properties as type β-collagenase (*9*). Since the bulk (∼90%) of the collagenases is the β type (Lane 5, Figure 1) and because of the similar kinetic properties of class I and II *C. histolyticum* collagenases, the two-enzyme reaction of type β- and δ-*C. histolyticum* collagenases are approximated with a single enzyme reaction model.

The proteolysis of collagens by a single collagenase can be written as the following chemical reactions:

$$C + E \underset{k_{-1}}{\overset{k_1}{\rightleftharpoons}} CE \xrightarrow{k_{cal}} P + E$$

where C, E, and CE are collagen I monomer, *C. histolyticum* collagenases, and collagen−collagenase complex, respectively, and *P* is the concentration of cleaved collagen fragments; their concentrations are denoted as [C], [E], and [CE], and k_1, k_{-1}, and k_{cal}, are the rate constants of the reactions.

These reactions can also be expressed in the form of following ordinary differential equations:

$$\frac{d[C]}{dt} = -k_1[C][E] + k_{-1}[CE] \quad (1)$$

$$\frac{d[CE]}{dt} = k_1[C][E] - (k_{-1} + k_{cal})[CE] \quad (2)$$

In our experiments, the initial conditions are $[C(t=0)] = C_0$ and $[CE(t=0)] = 0$, where C_0 is the amount or concentration of collagen coated on the mica surface. Since there was a large volume of collagenase containing buffer compared to the amount of collagen present, we can reasonably assume

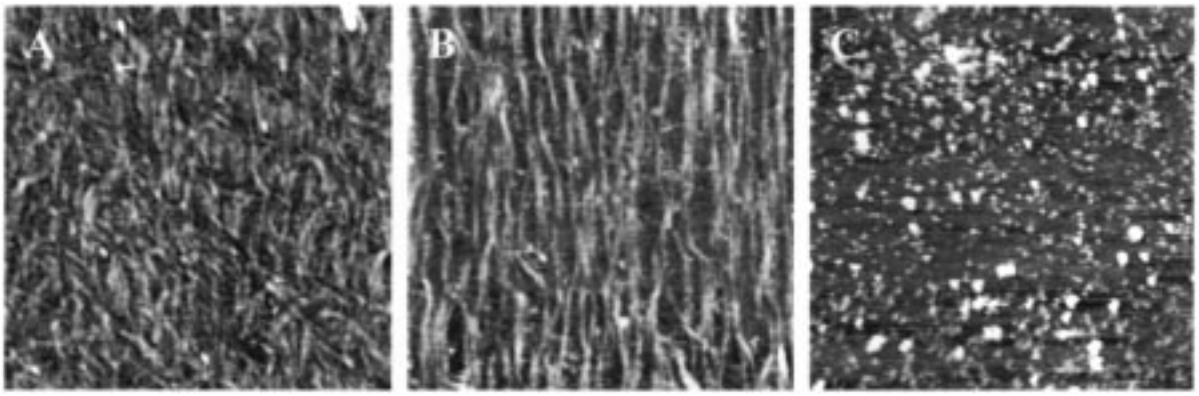

FIGURE 7: Inhibition of *C. histolyticum* collagenase in the Ca^{2+}-free/EDTA PBS imaged by tapping mode atomic force microscope. Collagen I molecules (A) prior to and (B) 30 min after they were perfused with 1 μg/mL *C. histolyticum* in calcium-free PBS containing 3 mM EDTA. Little collagen degradation was seen.(C) 30 min after Ca^{2+}-free/EDTA PBS was replaced with 1 μg/mL *C. histolyticum* in PBS containing 1 mM Ca. Collagen molecules was completely digested after the Ca^{2+} was added back. In this experiment, the solution change made between (A) and (B) caused AFM tip to disengage. The tip was re-engaged, before (B) was obtained, at a slightly different location on mica. Scan size: 2 μm $\times$ 2 μm.

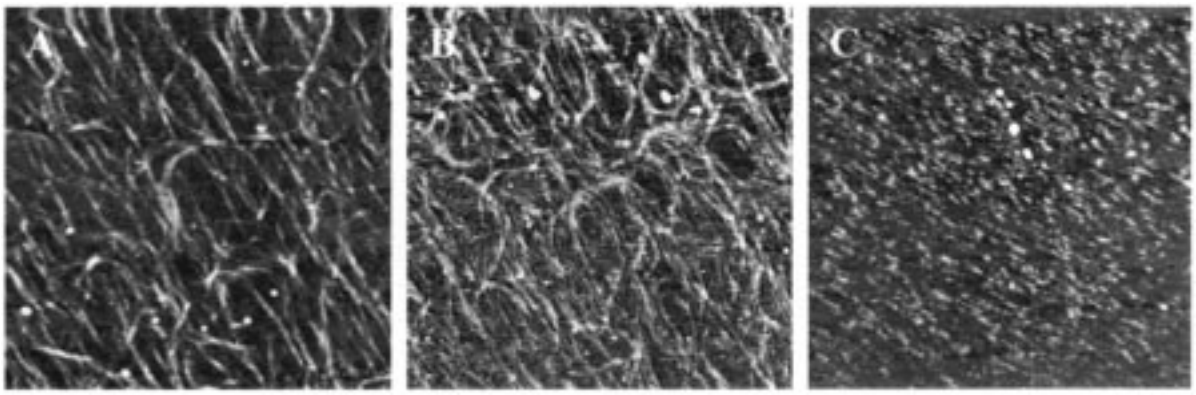

FIGURE 8: Inhibition of *C. histolyticum* collagenase by low pH. Collagen I molecules (A) prior to and (B) 30 min after they were perfused with 1 μg/mL *C. histolyticum* in PBS at pH 4.0. Most collagen molecules were digested (C) 30 min after pH was returned to 7.4, collagen molecules were completely digested. Scan size: 2 μm $\times$ 2 μm.

the concentration of free collagenase, [E], to be constant. With this assumption, equations (1) and (2) can be solved analytically,

$$[C(t)] = \frac{C_0}{2}\left[\left(1+\frac{k_{-1}+k_{cal}-k_1[E]}{\sqrt{(k_{-1}+k_{cal}+k_1[E])^2-4k_2k_1[E]}}\right)e^{-\lambda_1 t}+\left(1-\frac{k_{-1}+k_{cal}-k_1[E]}{\sqrt{(k_{-1}+k_{cal}+k_1[E])^2-4k_2k_1[E]}}\right)e^{-\lambda_2 t}\right]$$

$$[CE(t)] = \frac{C_0 k_1[E]}{\sqrt{(k_{-1}+k_{cal}+k_1[E])^2-4k_2k_1[E]}}(e^{-\lambda_1 t} - e^{-\lambda_2 t})$$

where

$$\lambda_1 = \frac{k_{-1}+k_{cal}+k_1[E]}{2} - \frac{1}{2}\sqrt{(k_{-1}+k_{cal}+k_1[E])^2-4k_2k_1[E]}$$

and

$$\lambda_2 = \frac{k_{-1}+k_{cal}+k_1[E]}{2} + \frac{1}{2}\sqrt{(k_{-1}+k_{cal}+k_1[E])^2-4k_2k_1[E]}$$

The amount/concentration of undigested collagen molecules, including those that form complexes with collagenase, is given by $[C(t)] + [CE(t)]$. The open squares in Figure 9 are the experimental data of $[C(t)] + [CE(t)]$, the number of intact collagen monomers on the imaged 2 $\times$ 2 μm^2 mica surface area, shown in Figure 3A−F. When k_{cal} is set between 500 hr^{-1} to 2000 hr^{-1} (*9*), the best estimate of $K_m = (k_{-1} + k_{cal})/ k_1$ is 0.9−3.8 μM by the nonlinear least-squares fitting of the experimental data with the analytical solution of equations (1) and (2). For k_{cal} = 1000 hr^{-1}, the previously measured value for β-*C. histolyticum* collagenase at r.t. (*9*), the best fit of the experimental data gives K_m = 1.9 μM. This best fit (k_{cal} = 1000 hr^{-1}, K_m = 1.9 μM, [E] = 20 nM (2 μg/mL and MW $\approx$ 100kD), and $k_{-1} = k_{cal}$) is plotted (solid line) in Figure 9 against the experimental data (open squares). The dashed line in Figure 9 represents a solution for [E] = 100 nM ($\sim$10 μg/mL collagenase) with the same K_m and k_{cal}, which is consistent with our observation that collagen molecules were completely degraded within 2 min when higher concentrations (10−100 μg/mL) of collagenase were added. These data are consistent with previously measured

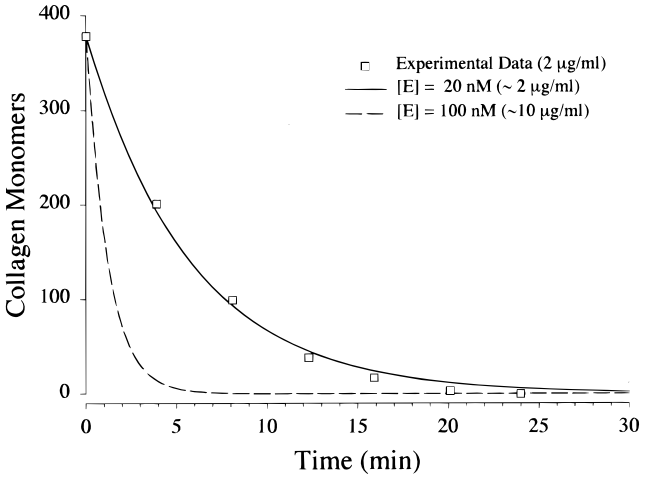

FIGURE 9: Experimental data fitted with known kinetic parameters of collagenases. The experimental data points (squares) were the total number of intact collagen I molecules in individual captured AFM images, as some of them were shown in Figure 3B−F. Since it took about 4 min to capture each image, their time points are average values. The fitted curves are the solutions of equations (1) and (2), $[C(t)]+[CE(t)]$, with $K_m = 1.9$ μM, $k_{cal} = k_{-1} = 1000$ hr^{-1}. The solid line has [E] = 20 nM, which resembles the experimental condition (~2 μg/mL collagenase). The dashed line represents [E] = 100 nM (~10 μg/mL collagenase) with $K_m = 1.9$ μM and $k_{cal} = 1000$ hr^{-1}; at this concentration, collagen molecules were promptly digested within a single frame (<4min).

kinetic parameters. In our experiments, *C. histolyticum* collagenases exhibit a slightly higher affinity (lower K_m, 1.9 vs 4 μM) or higher rate of hydrolysis (k_{cal}) compared to previous data of type β collagenase (*9*), which could be attributed to our under-estimation of the kinetic properties of type δ *C. histolyticum* collagenase.

The collagenase concentration used in our present study ranged mostly between 10 and 100 nM. On the basis of the differential equations (1) and (2) for reaction kinetics for these collagenase concentrations ($[E] \ll K_m$), when values of K_m and k_{cal} are set, the time course of the proteolysis reaction would not be significantly affected by changes in values of k_1 and k_{-1}, the rate constants for collagen/collagenase binding and dissociation. At low collagenase concentrations ($[E] \ll K_m$), multiple pairs of (K_m, k_{cal}) can lead to very similar reaction time courses (as the solid line plot in Figure 9). To independently determine the values of kinetic parameters K_m and k_{cal}, one needs to perform similar proteolysis experiments using several different concentrations of collagenase [E], especially at concentrations near K_m. However, because of the limited temporal resolution of the AFM, we cannot resolve the faster proteolysis reactions with high collagenase concentrations ($[E] \approx K_m$).

The rate constants for collagen/collagenase binding and dissociation, k_1 and k_{-1}, are not known. Though values of k_1 and k_{-1} did not significantly affect the experiments in our current study, they do have significant impact on the onset and the initial rate of the proteolysis at higher collagenase concentrations ($E \sim K_m$), especially for the first few seconds. The binding and dissociation rate constants also contain important information about the nature of collagen−collagenase interaction: e.g. if $k_{-1} \ll k_{cal}$, then collagenase binds tightly to a collagen molecule and binding will result in cleavage with near certainty. Our data (Figure 5A−C) suggest that a collagenase molecule may bind to and later dissociate from collagen molecules without cleavage. Our current experiments do not have the temporal resolution to resolve the first few seconds of the reactions and obtain the values for k_{-1} and k_{cal}, but atomic force microscope is an ideal tool to study protein−protein interactions at the molecular level using other approaches (*14*−*16*).

The present study provides the first images of single protein molecules being digested by a proteinase. By experimenting with different parameters, such as collagen-plating density, collagenase concentration, scanning speed, etc., it should be possible to obtain better images of collagen−collagenase complexes. The rate constant of collagen hydrolysis k_{cal} has been measured to be between 3 and 250 hr^{-1} for various tissue collagenases (*9*, *24*, *25*), which suggests that the reaction time for a single collagen cleavage ranges between 15 s to several minutes. The current AFM should be capable of capturing multiple snapshots of the slower collagenolysis reaction of single collagen−collagenase complexes. It should also be possible to image proteolysis and synthesis of more complex extracellular matrix molecules. With future improvement in image stability at a higher scanning speed, even the dynamics of the fast collagenolysis reactions can be unveiled at the scale of single molecules using atomic force microscopy. The multimodal imaging capability of AFM (*28*) will also allow for direct structure−function correlation studies of these macromolecules.

ACKNOWLEDGMENT

We thank Drs. Nils Almqvist, Ashok Parbhu, Arjan Quist, and Rajinder Bhatia for valuable technical advice, and Pete Sullivan for preparation of collagen I.

REFERENCES

1. Matrisian, L. M. (1990) *Trends Genet. 6*, 121−125.
2. Crawford, H. C., Matrisian, L. M. (1994−95) *Invasion Metastasis 14*, 234−45.
3. Gomez D. E., Alonso D. F., Yoshiji, H., and Thorgeirsson, U. P. (1997) *Eur. J. Cell Biol. 74*, 111−22.
4. Van der Rest, M., and Garrone, R. (1991) *FASEB J. 5*, 2814−23.
5. Brodsky, B., Tanaka, S., and Eikenberry, E. F. (1988) *Collagen.* Vol 1, pp 95−112, CRC Press, Boca Raton, FL.
6. Kielty, C. M., Kwan, A. P., and Holmes, D. F., Schor, S. L., and Grant, M. E. (1985) *Biochem. J. 227*, 545−54.
7. Mould, A. P., Holmes, D. F., Kadler, K. E., Chapman, J. A. (1985) *J. Ultrastruct. Res. 91*, 66−76.
8. Bond, M. D., and Van Wart, H. E. (1992) *J. Protein Chem. 11*, 99−107.
9. Mallya, S. K., Mookhtiar, K. A., and Van Wart, H. E. (1992) *J. Protein Chem. 11*, 99−107.
10. French, M. F., Bhown, A., Van Wart, H. E. (1992) *J. Protein Chem. 11*, 83−97.
11. Lal, R., and John, S. A. (1994) *Am. J. Physiol. 266* (1 Pt. 1), C1−21.
12. Lal, R. (1996) *Scanning Microsc. 10*, 81−96.
13. Yang, J, and Shao, Z. F. (1995) *Micron. 26*, 35−49.
14. Moy, V. T., Florin, E. L., and Gaub, H. E. (1994) *Science 266*, 257−9.
15. Lee, G. U., Chrisey, L. A., and Colton, R. J. (1994) *Science 266*, 771−3.
16. Hinterdorfer, P., Baumgartner, W., Gruber, H. J., Schilcher, K., and Schindler, H. (1996) *Proc. Natl. Acad. Sci. U.S.A. 93*, 3477−81.
17. Guthold, M., Bezanilla, M., Erie, DA., Jenkins, B., Hansma, H. G., and Bustamante, C. (1994) *Proc. Natl. Acad. Sci. U.S.A. 91*, 12927−31.

18. Shattuck, M. B., Gustafsson, M. G., Fisher, K. A., Yanagimoto, K. C., Veis, A., Bhatnagar, R. S., and Clarke, J. (1994) *J. Microsc. 174* (Pt 1), RP1−2.
19. Wolberg, A. S., Stafford, D. W., and Erie, D. A. (1997) *J. Biol. Chem. 272*, 16717−20.
20. Brodsky, B., and Eikenberry, E. F. (1982) *Methods Enzymol. 82* Pt A, 127−74.
21. Laemmli, U.K. (1970) *Nature 227*, 680−5.
22. Shroff, S. G, Saner, D. R, and Lal, R. (1995) *Am. J. Physiol. 269*, C286−C292.
23. Emod, I., Tong, N. T., and Keil, B. (1981) *Biochim. Biophys. Acta 659*, 283−91.
24. Soru, E., and Zaharia, O. (1972) *Enzymologia 43*, 45−55.
25. Van Wart, H. E., and Steinbrink, DR. (1985) *Biochemistry 24*, 6520−6.
26. Hasty, K. A., Jeffrey, J. J., Hibbs, M. S., and Welgus, H. G. (1987) *J. Biol. Chem. 262*, 10048−52.
27. Welgus, H. G., Jeffrey, J. J., and Eisen, A. Z. (1981) *J. Biol. Chem. 256*, 9511−5.
28. Lal, R., and Proksch, R. (1997) *Int. J. Imaging Syst. Technol. 8*, 293−300.

BI990800Q